ISSN: 2366-1313

DESIGN OPTIMIZATION OF TRANSFORMER USING CONVENTIONAL METHOD

[1] Mohammed Iliyas, [2] Dr. Jai Veer Singh
[1] Research Scholar of OPJS University, Churu, Rajasthan
[2]Associate Professor, OPJS University, Churu, Rajasthan

Abstract
The conventional approach to Transformer Design Optimization is used in this chapter. A heuristic strategy that assigns various design variables to various alternative designs is essentially what this method is. Finally, the design that solves all issues with minimal electrode material manufacturing costs (aluminium and CRGO costs) is selected.

Keywords: Artificial Intelligence, Transformer Design Optimization, NSGA,

1. Introduction

Manufacturers need to design the best (optimal) technology for the current adaptation of new legislation involving the use of high-efficiency supply transformers because it would be difficult to ask consumers in today's highly dynamic retail environment to fully pay for the consequent rise in product prices.

With dynamic and discontinuous goal features and constraints that fully identify transformer characteristics in accordance to domestic or external requirements as well as user expectations, Transformer Design Optimization is a non-linear mixed integer programming problem.

This literature describes a variety of trustworthy functions, but the most generally used ones are those that reduce the TOC transformer's manufacturing costs while maintaining its lifetime cost (i.e. the total cost of ownership). Minimizing major content costs, production expenses, and TOC are the three functionality goals offered in the study's package. Tocs are required by rules yet regulatory agencies are urged to continue utilising them since the guidelines merely seek to raise transformational efficiency's minimal minimum level (Global Industry Analysts 2014.). Transmission lines and transformer architectural efficiency are two topics that have received a lot of attention in the literature. First, a review of the literature conducted in 2009 (Amoiralis IE 2014) provided broad outlines of transformer design and optimization progress during the previous 35 years based on more than 420 papers, 50 transformer-related books, and 65 recommendations. The research article might need further investigations on transformer architecture and transformer design optimization (Olivares-Galvan JC 2001, Amoiralis EI 2009, Energy Efficient Transformer Solutions 2014.).

ISSN: 2366-1313

Several methods to its attainment have still to be investigated, as noted in the literature, when it comes to global optimization of disruptive architecture, European Copper Institute (2014).

2. Review Of Literature

El-Taweel and Hewidy(2004) proposed that a planetary EDM be used to achieve greater surface completion and dimensional precision at the time of employment shortened. A few reports have covered the proposed model and identified the optimal work atmosphere for machining processes for parts such as AISI D2, wire grids and copper cathode clay composite materials. Many researchers have obtained managed cryogenic hardware and workpiece cooling to make remarkable changes in the machining process execution. The ordinary EDM process is calledcryo-rewarded EDM, at the stage where certain methodologies apply to hardware cooling and job content.

According to Kapoor et al. (2012), this kind of metal wire for cryogenically frozen clearing between beatings and stresses is the key technique variable.

Both Gill and Singh are in this grouping (2010) The electronic discharge stage uses a cryogenically rewarded titanium compound piece with efficient copper terminal preparation. Higher MRR with completely penetrated panels and decreased wear rate will be achieved via cryogenically freezing the working material.

Pandey and Srivastava (2012) Anode wear and surface differential were found to be significantly reduced with higher surface resistance using a cryogenically corrected copper machine on a steel-grade M 2 computer.

Specifically, the impacts of dispersed graphite particles on execution stages were examined by Kumar et al. (2011) using data from experiments with large variables in this direction. When using cryogenically rewarded material for copper instruments, the wear ratio and TWR of Inconel 718 were dissolved.

Karthikeyan et al. (2015) have studied the enhancement of transient protection across the perfect field and STATCOM reversal. The STATCOM presentation is modified by using a non-linear time-space replication. The result indicates that the optimal field and tuning of STATCOM influences the transient solidity enhancement system.

3. METHODOLOGY

This approach optimizes the transformer architecture with the following technological features:
1) Oil-immersed transformers in three stages.
2) Main style transformer magnetic circuit.

ISSN: 2366-1313

3) Rectangular wire made of two LV conductors strips and circular HV conducers cross section. The programming software requires several differences of architecture variables into consideration. These differences cause a candidate solution to be examined. In every one of the nominee solutions, the cost of the active components and the required solution can be measured if all conditions are met. Finally, the transformer with the lowest development costs and the optimal transformer is chosen from the appropriate solutions.

Four factors of judgement have been considered

1. Constant importance of K
2. Maximum density value of flowB_m
3. Present density valueδ_{HV}in HV winding.
4. 5. Present density valueδ_{LV}in LV winding.

Giving K, B_m , $\delta_{HV}$and δ_{LV}separate values are determined from a list: loops = different values k* Numbers of the values B_m *No. The complete candidate solutions are calculated from the following sequence. Present density values δ_{HV} in HV *No winding. of the current δ_{LV}in LV winding density values. For the phase size of 0.01, 16 different K values, 5 different B_m, density values, and 5 different existing $\delta_{LV}$and δ_{HV}values in LV and HV are taken into consideration in the programme. The cumulative number of prototypes measured in this plan, thus, corresponds to $16 \times 51 \times 5 \times 5 = 20400$. Figure 3.1 displays the simpler flowchart to minimise the active component costs

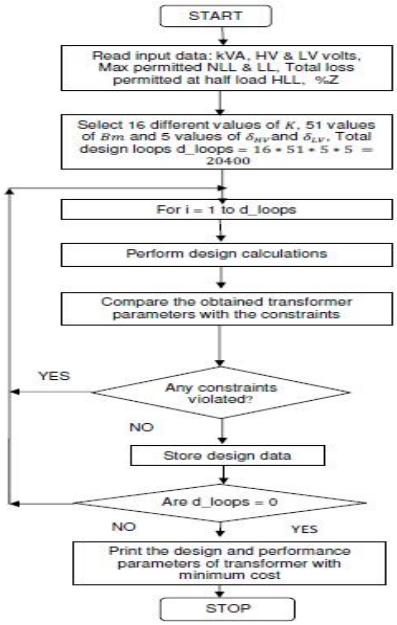

Figure 3.

1 Flowchart for Optimum Transformer Design using ESM

ISSN: 2366-1313

3.1 STEPS INVOLVED IN TRANSFORMER DESIGN

This section explains the architecture methodology of a three-phase core 100 kVA transformer. Aluminum and HV coils are affected by aluminum conducers because aluminum for transformers less than 190 kVA is cheaper than copper (75).

3.1.1 Calculation of Number of Turns for LV and HV

The transformer equation is used to calculate the voltage per switch, $E_t = K\sqrt{Q}$, where E t is volt by turn and K is always provided

$$K = \sqrt{\frac{4.44 * f * \emptyset m}{AT * 10^3}} \qquad 3.1$$

The amount of LV (NLV) and HV (NHV) rotations is defined below:

$$N_{LV} = \frac{V_{LV}}{\sqrt{3} * E_t}$$

$$N_{HV} = \frac{\sqrt{3} * V_{HV} * N_{LV}}{V_{LV}}$$

3.1.2 Diameterand Core Area

The equation describes the gross core area

$$A_g = \frac{E_t * 10^2}{2.22 * B_m * k_f} \qquad 3.2$$

The value of k_f (stacking factor) is 0.97. The transformer diameter is obtained from 9-step Centre (77).

$$d_c = \sqrt{\frac{A_g * 4}{\pi * 0.935}} \qquad 3.3$$

The middle diameter of Equation 3.3 is then completed at the nearest value.

3.1.3 Core Weight and Expense Estimate

The core weight of the transformer is dependent on (77)

$$w_c = (4 * Cl_c + 3 * H_w) * A_g * k_f * \rho c \qquad \ldots 3.4$$

The central cost is then achieved by multiplying the appropriate cost coefficient by the core weight.

ISSN: 2366-1313

3.1.4 Cost and Conductor Weight

The total LV/HV winding diameter and the overall amount of turns, cross-sectional area and winding material decide the combined weight of the driver inside the converter. It is supplied by

$W_{al} = 3 * \rho_{AL} * \pi * (2 * MD_{LV} * N_{LV} * A_{LV} + MD_{HV} * N_{HV} * A_{HV}) * 10^{-6} \ldots 3.5$

The expense will be determined by combining it with an acceptable cost coefficient after the winding weight is reached. Equation 3.5 indicates factor 2 as two strips of LV are included.

3.1.5 Load Losses of LV and HV Winding

The following equations calculate LV and HV winding losses

$$LL_{LV} = \frac{3*I_{LV}^2*\pi*MD_{LV}*N_{LV}*\rho_R}{A_{LV}} \qquad 3.6$$

$$LL_{HV} = \frac{3*I_{LV}^2*\pi*MD_{LV}*N_{LV}*\rho_R}{A_{HV}} \qquad 3.7$$

The absolute depletion of complete load$W_{FL}$is received from then

$W_{FL} = LL_{LV} + LL_{HV}$ 3.8

3.1.6 No-load Loss and No-load Current Calculation

The core loss curve for M4 grade material which gives specific no load loss $W_{nlsp}$and specific exciting power requirement W_{esp}at different values of flux density is obtained using neural networks as discussed in previous study. The total no-load loss and exciting power is then obtained by

$W_{NL} = W_{nlsp} * W_c$ 3.9

$W_e = W_{esp} * W_c$3.10

As shown below, magnetization, core failure and no load current are achieved

$I_\mu = (W_e * W_c)/(\sqrt{3} * V_{LV})$ 3.11

$I_w = W_{NL}/(\sqrt{3} * V_{LV})$ 3.12

$$I_0 = \sqrt{I_\mu^2 + I_w^2} \qquad 3.13$$

3.1.7 Response, Resistance and Impedance Percentage

ISSN: 2366-1313

The response, intensity and impedance levels are defined by the following:

$$\%X = \frac{7.91 * f * I_{LV} * N_{LV}^2 * \pi * D_m}{V_{LV} * A_{sl} * 10^6} * (\alpha + \frac{R_{BHV} + R_{BLV}}{3}) \quad 3.14$$

$$\%R = (LL_{LV} + LL_{HV}) * \frac{100}{Q} \quad 3.15$$

$$\%Z = \sqrt{\%X^2 + \%R^2} \quad 3.16$$

3.1.8 Efficiency and Voltage Regulation

Output η at full power factor capacity$\cos\phi$is given by

$$\eta = \frac{Q * cos\phi}{Q * cos\phi + W_{NL} + W_{HL}} \quad 3.17$$

The voltage regulator V_r with various power factor values is defined

$$\%V_r = \%R * cos\emptyset + \%X * sin\emptyset \quad 3.18$$

3.1.9 Calculation of First peak of Asymmetrical Short Circuit Current

The equation gives the first peak value of asymmetrical short circuit for LV and HV

$$I_{asc} = K * \sqrt{2I_{ph}/\%Z} \quad 3.19$$

Here I_{ph} is phase current in Amperes and K is a function of the ratio of %X and%R, which is obtained from IS 2026,

3.1.10 Calculation of Asymmetrical Short Circuit Ampere Turns

The value of asymmetrical short circuit ampere turns for LV and HV windings are obtained as

$$ASCAT_{LV} = N_{LV} * I_{ASCLV} \quad 3.20$$

$$ASCAT_{HV} = N_{HV} * I_{ASCHV} \quad 3.21$$

3.1.11 Hoop Stress

Hoop stress is mechanical stress acting circumferentially perpendicular to both the axis and the windings. The value of hoop stress induced in LV and HV windings during short circuit conditions is obtained using the equation

ISSN: 2366-1313

$$HP_{LV} = {K_h * I_{LV}^2 * R_{LV}}/{H_w * \%Z^2} 3.22$$

$$HP_{HV} = {K_h * I_{HV}^2 * R_{HV}}/{H_w * \%Z^2} 3.23$$

The value of K_h obtained from (86) is given by $K_h = 0.02 * (\frac{K * \sqrt{2}}{2.55})^2$

3.1.12 Radial Bursting Force

These forces tend to increase the distance between the windings and causes damage to the windings

Radial bursting force in LV and HV windings is calculated using the equations

$$F_{RHV} = \frac{(2 * \pi * H\rho_{mean} * I_{HV}^2 * N_{HV})}{\delta_{HV}} \quad ...3.24$$

$$F_{RLV} = \frac{(2 * \pi * H\rho_{mean} * I_{LV}^2 * N_{LV})}{\delta_{LV}} \quad 3.25$$

Here $H\rho_{mean}$ is the average value of HP_{HV} and HP_{LV} obtained in section 3.2.11

3.1.13 Internal Axial Compression

The adjacent turns of windings experience attractive force. This axial force bends the winding in vertical direction. It is given by

$F_c = \frac{34 * Q}{\%Z * H_w} 3.26$

3.1.14 Average Temperature of Winding after Short Circuit

The duration of short circuit current I_{SC} to be used for calculation of thermal ability to withstand short circuit current should be 2 sec, unless different condition is specified. The average temperature θ_1 of each winding after loading with symmetrical short circuit current I_{SC} for duration of time)tseconds is given by

$$\theta_1 = \theta_0 + \frac{(2 * \theta_0 + 225)}{{45700}/{t * J_{SC}^2 - 1}} \quad \ldots 3.27$$

3.1.15 Magnetizing Current Inrush

Magnetizing current inrush is the current which flows in the transformer primary when it is switched on to the supply. The magnetizing current inrush in HV is given by

ISSN: 2366-1313

$$I_{\mu R} = \frac{H_w * A_i\,(2*B_m + B_r - 2.2)*10^{-4}}{N_{HV} * A_{HV} * \mu_0} \ldots 3.28$$

4. Result and Findings

This paper explores the effects of the Transformer Interface Optimization (TDO) issue by Exhaustive Search Process (ESM). The shortcomings of no load failure, loss of loads, loss of percent, and total losses for half load transformers for the 1st and 2stars as well as other software parameters were set out in Table 3.1 according to the Energy Efficiency Office (78).

Table 3.1 Input Parameters for 1-Star and 2-Star Rated Transformers

Sr. No.	Parameter	1-star	2•star	Units
1	Rated power	100	1 00	kVA
2	Max. Total Losses permitted	2020	1910	W
3	Max. Losses permitted at half load	700	610	W
4	Max. No load losses permitted	220	200	W
5	Max. Percentage impedance permitted	4.7	4.7	%
6	Rated low voltage	433	433	H
7	Rated high voyage	11000	11000	H
8	Permitted Temperature rise	S0	50	"C

Tables 3.2 and 3.3 Exemplify 100kVA11/0.433kV, Transmission Transformer, output of 1-star and 2-star.

Table 3.2 Sample of Accep table Solutions Pertaining to 1-Star Rating

Active Part Cost (INR)	No-load losses (W)	Load losses (W)	%Z	Efficiency
59608	187.19	1760.67	4.27	98.089
61632	189.61	1675.74	4.53	98.168
59564	187.19	1767.69	4.27	98.082
61351	188.70	1683.01	4.55	98.162
59284	186.29	1774.71	4.29	98.076
61307	188.70	1690.27	4.55	98.155
59242	186.29	1781.72	4.29	98.069
61263	188.70	1697.54	4.55	98.148
61263	188.70	1697.54	4.55	98.148
59199	186.29	1788.74	4.30	98.063

ISSN: 2366-1313

61208	190.88	1664.51	4.51	98.178
59146	188.45	1756.26	4.26	98.092
58825	187.53	1770.27	4.28	98.079
67707	216.64	1505.61	3.55	98.306
69698	219.65	1427.22	3.75	98.379
68741	212.63	1531.47	3.57	98.285

Total number of designs = 20400
Rejected cumulative designs for infringement of restrictions= 13403
Accepted cumulative prototypes = 6997
Design no. from all prototypes picked = 1178
Design no. selected from all shortlisted designs = 15
Table 3.3 Sample of Acceptable Solutions Pertaining to 2-Star Rating

Part Cost (INR)	No-load losses (W)	Load losses (W)	%Z	Efficiency
59529	183.16	1706.80	4.61	98.145
63804	177.02	1707.04	4.59	98.150
63377	178.26	1702.74	4.58	98.153
62877	179.25	1698.50	4.57	98.156
61931	181.62	1697.50	4.55	98.155
61650	180.76	1704.86	4.57	98.149
61251	182.15	1700.73	4.56	98.151
61206	182.15	1708.07	4.56	98.144
71517	198.61	1628.94	3.86	98.205
70891	199.53	1624.28	3.85	98.208
64972	199.67	1624.02	3.87	98.208
58272	194.91	1654.76	4.45	98.183
57921	196.83	1651.04	4.44	98.185
65877	196.35	1615.72	3.86	98.220
67898	199.01	1533.85	4.08	98.296
66857	192.26	1630.86	3.88	98.209

Total number of designs = 20400
Total solutions rejected = 18379
Total solutions accepted = 2021
Design no. selected from all total designs = 5626
Design no. selected from all short listed designs = 63
The designs that exceed the restrictions shall be refused and the costs of all appropriate alternatives, including the transformer configuration and output criteria, shall be written on the

ISSN: 2366-1313

control window. The cheapest active component, design measurements, technological and dynamic Table 3.4 and table 3.5 display the efficiency characteristics of 100 kVA, 11/0.433 kV transformers.

Table 3.4 1-Star and 2-Star Ranking Transformer Key architecture dimensions and efficiency parameters

Parameter	1-star rating	2-star rating	Units
Cheapest cost	46579	58702	INR
Flux density	1.67	1.41	T
Axial length of HV coil	448	400	mm
Gross core area	88.98	118.56	cm^2
Distance between adjacent core centers	252	277	mm
Window height	518	470	mm
Core weight	169.16	221.53	kg
Conductor weight	62.45	68.81	kg
Tank length	793	868	mm
Tank breadth	319	344	mm
Tank height	917	901	mm
No load losses	219.43	195.11	W
Total losses	2016.48	1853.73	W
Total losses at half load	668.70	609.74	W
Percentage impedance	4.376	4.458	%
Efficiency (full load, upf)	98.02	98.18	%

If the manufacturer needs a minor change in the measurements of the software configuration of the transformers, the software should join alternate values of the allowable no load and lack of load as long as the restriction referred to in Table 3.1 is not violated.

5. CONCLUSION

This segment explores systematically all application choices by dismissing all applicant alternatives (designs) that breach consumer limitations. The software then proposes all acceptable choices and offers the best design and output parameters of the transformer. The presented approach is useful for delivery transformer manufacturers since it saves significant

design time. However, it should be noted that it is not possible to go below step size of 0.01 for design variables, as it would increase the execution time tremendously.

REFERENCES

1. Ibtissem, L.Noureddine and B. Pierre, "Tuning PID controller using multi-objective Ant Colony Optimization", Applied computational intelligence and soft computing journal, Vol. 2012, pp. 1-7.

2. [13] M. Peyvandi, M. Zafarani and E. Nasr (2011) "Comparison of Particle Swarm Optimization and Genetic algorithm in Improving Power System Stability by an SSSC base Controller," Journal of Electrical Engineering and Technology, Vol. 5, No. 2.

3. Mostafa Abdollahi*, SaeidGhasrdashti, Hassan Saeidinezhad and FarzadHosseinzadeh (2013) "Optimal PSS Tuning by using Artificial Bee Colony", Journal of Novel Applied Sciences, Journal-2013-2-10/534-540 ISSN 2322-5149

4. FunsoAriyo, Michael Omoigui (2012) "Investigation of the Damping of Electromechanical Oscillations Using Power System Stabilizers (PSS) in Nigerian 330 kV Electrical Network", Electrical and Electronic Engineering 2(4):236-244

5. K.Karthikeyana*,P.K.Dhalb (2015) Transient Stability Enhancement by Optimal Location and Tuning of STATCOM using PSO, Published by Elsevier, 21, pp 345 – 351

6. Prabhu S, Vinayagam BK (2011) AFM surface investigation of Inconel 825 with multi wall carbon nano tube in electrical discharge machining process using Taguchi analysis, Archives of Civil and Mechanical Engineering, 11(1): 149-169.

7. Ebeid SJ, Hewidy MS, El-Taweel TA, Youssef AH (2004) Towards higher accuracy for ECM hybridized with low-frequency vibrations using the response surface methodology, Journal of Materials Processing Technology, 149(1), 432-438

8. Kumar A, Maheshwari S, Sharma C, Beri, N (2011) Analysis of machining characteristics in additive mixed electric discharge machining of nickel-based super alloy Inconel 718, Materials and Manufacturing Processes, 26(8): 1011-1018.

9. Jafferson JM, Hariharan P (2013) Machining performance of cryogenically treated electrodes in microelectric discharge machining: A comparative experimental study, Materials and Manufacturing Processes, 28(4): 397-402.

10. Jatinder Kapoor1, Sehijpal Singh1, Jaimal Singh Khamba (2012) Effect of cryogenic treated brass wire electrode on material removal rate in wire electrical discharge machining, Volume: 226 issue: 11, page(s): 2750-2758

ISSN: 2366-1313

11. Gill, SS, Singh, J. (2010) Effect of deep cryogenic treatment on machinability of titanium alloy (Ti-6246) in electric discharge drilling. Mater Manuf Process, 25: 378–385.

12. Srivastava V., Pandey P.M. (2012) Performance evaluation of electrical discharge machining (EDM) process using cryogenically cooled electrode. Mater. Manuf. Process;27:683–688.

13. Mohanty, S.; Mishra, A.; Nanda, B.K.; Routara, B.C. (2018) Multi-objective parametric optimization of nano powder mixed electrical discharge machining of AlSiCp using response surface methodology and particle swarm optimization. Alexandria Eng. J., 57, 609–619.

14. Chen Y, Mahdivian SM (2000) Analysis of electro-discharge machining process and its comparison with experiments. J Mater Process Technol 104(1):150–157

15. AmareshSahua , SabyasachiPattnaikb (2016) "Evolving Neuro Structure Using Adaptive PSO and Modified TLBO for Classification" AmareshSahu and SabyasachiPattnaik / Procedia Computer Science 92 (2016) 450 – 454.

16. Sidhu T.S., Gill H.S. and Sachdev M.S. (1999), 'A Power Transformer Protection Technique with Stability during Current Transformer Saturation and Ratio-Mismatch Conditions', IEEE Transactions on Power Delivery, Vol. 14, No. 3, pp. 798-804

17. [91] J. S. R. Jang, "ANFIS: Adaptive-network-based fuzzy inference systems," IEEE Trans. on Syst., Man and Cybern., vol. 23, no. 3, pp. 665–684, May/June 1993.

18. Glover, F. (1986) "Future Paths for Integer Programming and Links to Artificial Intelligence," Computers and Operations Research, Vol. 13, pp. 533-549.

19. Glover, F. and Laguna, M., (1997). Tabu Search, Kluwer Academic Publishers, Boston.

20. M. Dorigo. 1992. Optimization, Learning and Natural Algo-rithms (in Italian). Ph.D. thesis, Dipartimento di Met-tronica, Politecnico di Milano, Italy.

21. Storn, R., and Price, K., (1997), "Differential Evolution - A Simple and Efficient Heuristic for Global Optimization over Continuous Spaces," Journal of Global Optimization, Vol. 11, No. 4, pp. 341-359.